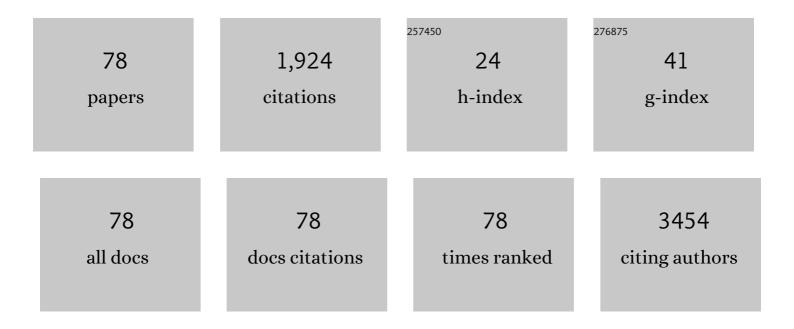
Dandan Song

List of Publications by Year in descending order

Source: https://exaly.com/author-pdf/4813702/publications.pdf Version: 2024-02-01



#	Article	IF	CITATIONS
1	Improved phase purity and film quality in quasi-2D perovskite light-emitting diodes by an additive with the trimethacrylate group. RSC Advances, 2022, 12, 3081-3089.	3.6	7
2	Suppressed Halide Segregation and Defects in Wide Bandgap Perovskite Solar Cells Enabled by Doping Organic Bromide Salt with Moderate Chain Length. Journal of Physical Chemistry C, 2022, 126, 1711-1720.	3.1	8
3	Highly efficient CIGS solar cells based on a new CIGS bandgap gradient design characterized by numerical simulation. Solar Energy, 2022, 233, 337-344.	6.1	29
4	Predicting the photon energy of quasi-2D lead halide perovskites from the precursor composition through machine learning. Nanoscale Advances, 2022, 4, 1632-1638.	4.6	6
5	Stable and Efficient Red-Emitting Perovskite Cross-Shaped Nanoplates. Journal of Physical Chemistry Letters, 2022, 13, 1506-1511.	4.6	3
6	Device performance improvements in all-inorganic perovskite light-emitting diodes: the role of binary ammonium cation terminals. Physical Chemistry Chemical Physics, 2022, 24, 6208-6214.	2.8	2
7	Key Factors Governing the External Quantum Efficiency of Thermally Activated Delayed Fluorescence Organic Light-Emitting Devices: Evidence from Machine Learning. ACS Omega, 2022, 7, 7893-7900.	3.5	11
8	Small dose of phosphorescent dopant enabling high efficiency and bright solution-processed sky-blue organic light-emitting diodes. Optical Materials, 2022, 128, 112278.	3.6	1
9	Modification of PEDOT: PSS to enhance device efficiency and stability of the Quasi-2D perovskite light-emitting diodes. Organic Electronics, 2022, 108, 106579.	2.6	8
10	Highâ€Performance MAPbI ₃ /PM6:Y6 Perovskite/Organic Hybrid Photodetectors with a Broadband Response. Advanced Optical Materials, 2022, 10, .	7.3	9
11	The recombination zone adjusted by the gradient doping of TPA-DCPP for efficient and stable deep red organic light emitting diodes. RSC Advances, 2021, 11, 24436-24442.	3.6	3
12	Key factors governing the device performance of CIGS solar cells: Insights from machine learning. Solar Energy, 2021, 228, 45-52.	6.1	14
13	Bandgap tuning strategy by cations and halide ions of lead halide perovskites learned from machine learning. RSC Advances, 2021, 11, 15688-15694.	3.6	36
14	High-Performance Near-Infrared Photodetectors Based on the Synergy Effect of Short Wavelength Light Filter and Long Wavelength Response of a Perovskite/Polymer Hybrid Structure. ACS Applied Materials & Interfaces, 2021, 13, 61818-61826.	8.0	7
15	Investigation on light-induced storage of charges with capacitance/conductance-voltage and its frequency characteristics. Organic Electronics, 2020, 76, 105425.	2.6	6
16	Filterless narrowband photodetectors employing perovskite/polymer synergetic layers with tunable spectral response. Organic Electronics, 2020, 76, 105417.	2.6	29
17	Enhanced <i>V</i> _{OC} of two-dimensional Ruddlesden–Popper perovskite solar cells using binary synergetic organic spacer cations. Physical Chemistry Chemical Physics, 2020, 22, 54-61.	2.8	15
18	Solvent modification to suppress halide segregation in mixed halide perovskite solar cells. Journal of Materials Science, 2020, 55, 9787-9794.	3.7	7

#	Article	IF	CITATIONS
19	Managed carrier density and distribution in solution-processed emission layer to achieve highly efficient and bright blue organic light-emitting devices. Organic Electronics, 2020, 82, 105703.	2.6	5
20	Improved film morphology and reduced defects in solution-processed red phosphorescent emission layer of the organic light-emitting diodes. Synthetic Metals, 2020, 261, 116322.	3.9	2
21	Synergetic interface and morphology modification to achieve highly efficient solution-processed sky-blue organic light-emitting diodes. Organic Electronics, 2020, 83, 105721.	2.6	5
22	Interface energy level alignment and improved film quality with a hydrophilic polymer interlayer to improve the device efficiency and stability of all-inorganic halide perovskite light-emitting diodes. Journal of Materials Chemistry C, 2020, 8, 6743-6748.	5.5	12
23	The improved performance and mechanism of solution-processed blue PhOLEDs based on double electron transport layers. RSC Advances, 2020, 10, 13215-13222.	3.6	19
24	Investigation on OLEDs efficiency roll-off with interfacial charge storage and their time-resolved emission spectra. Organic Electronics, 2020, 83, 105756.	2.6	10
25	Solvent treatment induced interface dipole and defect passivation for efficient and bright red quantum dot light-emitting diodes. Organic Electronics, 2019, 75, 105412.	2.6	8
26	Investigating the evolution of excitons in polymer light-emitting diodes by transient measurement. Organic Electronics, 2019, 68, 45-49.	2.6	8
27	Benefits of the Hydrophobic Surface for CH3NH3PbI3 Crystalline Growth towards Highly Efficient Inverted Perovskite Solar Cells. Molecules, 2019, 24, 2027.	3.8	16
28	Highly efficient and bright blue organic light-emitting devices based on solvent engineered, solution-processed thermally activated delayed fluorescent emission layer. Organic Electronics, 2019, 71, 1-6.	2.6	14
29	Highly bright perovskite light-emitting diodes based on quasi-2D perovskite film through synergetic solvent engineering. RSC Advances, 2019, 9, 8373-8378.	3.6	15
30	Improved carrier injection and balance in solution-processed blue phosphorescent organic light emitting diodes based on mixed host system and their transient electroluminescence. Synthetic Metals, 2019, 252, 15-20.	3.9	13
31	Lead-Halide Perovskite as the Host Material for Solution-Processed Phosphorescent Organic Light-Emitting Diodes. Journal of Physical Chemistry C, 2019, 123, 30099-30105.	3.1	4
32	Investigating the evolution of exciplex states in thermally activated delayed fluorescence organic light-emitting diodes by transient measurement. Journal of Luminescence, 2018, 201, 38-43.	3.1	13
33	Improving the photovoltaic performance of planar heterojunction perovskite solar cells by mixed solvent vapor treatment. RSC Advances, 2018, 8, 11574-11579.	3.6	8
34	Morphology Optimization of Silver Nanoparticles Used to Improve the Light Absorption in Thin-Film Silicon Solar Cells. Plasmonics, 2018, 13, 555-561.	3.4	7
35	Highly bright and stable all-inorganic perovskite light-emitting diodes with methoxypolyethylene glycols modified CsPbBr3 emission layer. Applied Physics Letters, 2018, 113, .	3.3	26
36	3.5: Investigation of excitedâ€state dynamics upon both photo―and electroâ€excitation of thermally activated delayed fluorescent molecules. Digest of Technical Papers SID International Symposium, 2018, 49, 29-34.	0.3	0

#	Article	IF	CITATIONS
37	Investigation of excitedâ€state dynamics upon both photoâ€excitation and electroâ€excitation of thermally activated delayed fluorescent molecules. Journal of the Society for Information Display, 2018, 26, 694-699.	2.1	2
38	Improving charge transport by the ultrathin QDs interlayer in polymer solar cells. RSC Advances, 2018, 8, 17914-17920.	3.6	5
39	Improving the Charge Carrier Transport and Suppressing Recombination of Soluble Squaraine-Based Solar Cells via Parallel-Like Structure. Materials, 2018, 11, 759.	2.9	9
40	Biphenyl Triarylamine Hole Transport Material for Highly Efficient and Low-Temperature Solution-Processed <i>p</i> – <i>i</i> – <i>n</i> Perovskite Solar Cells. Journal of Nanoscience and Nanotechnology, 2018, 18, 7374-7379.	0.9	2
41	Highly Efficient Electronâ€Selective Layer Free Perovskite Solar Cells by Constructing Effective p–n Heterojunction. Solar Rrl, 2017, 1, 1600027.	5.8	82
42	A TiO ₂ embedded structure for perovskite solar cells with anomalous grain growth and effective electron extraction. Journal of Materials Chemistry A, 2017, 5, 1406-1414.	10.3	59
43	Postsynthetic, Reversible Cation Exchange between Pb ²⁺ and Mn ²⁺ in Cesium Lead Chloride Perovskite Nanocrystals. Journal of Physical Chemistry C, 2017, 121, 20387-20395.	3.1	63
44	Degradation of organometallic perovskite solar cells induced by trap states. Applied Physics Letters, 2016, 108, .	3.3	37
45	Dual function interfacial layer for highly efficient and stable lead halide perovskite solar cells. Journal of Materials Chemistry A, 2016, 4, 6091-6097.	10.3	90
46	Bunchy TiO2 hierarchical spheres with fast electron transport and large specific surface area for highly efficient dye-sensitized solar cells. Nano Energy, 2016, 23, 122-128.	16.0	34
47	Etching anisotropy mechanisms lead to morphology-controlled silicon nanoporous structures by metal assisted chemical etching. Nanoscale, 2016, 8, 3085-3092.	5.6	30
48	Photo-induced degradation of lead halide perovskite solar cells caused by the hole transport layer/metal electrode interface. Journal of Materials Chemistry A, 2016, 4, 1991-1998.	10.3	90
49	A comparison of light-harvesting performance of silicon nanocones and nanowires for radial-junction solar cells. Scientific Reports, 2015, 5, 11532.	3.3	53
50	Smart Hybrids of Zn ₂ GeO ₄ Nanoparticles and Ultrathin g ₃ N ₄ Layers: Synergistic Lithium Storage and Excellent Electrochemical Performance. Advanced Functional Materials, 2015, 25, 6858-6866.	14.9	182
51	Co-catalytic mechanism of Au and Ag in silicon etching to fabricate novel nanostructures. RSC Advances, 2015, 5, 96483-96487.	3.6	11
52	DMSO-based PbI ₂ precursor with PbCl ₂ additive for highly efficient perovskite solar cells fabricated at low temperature. RSC Advances, 2015, 5, 104606-104611.	3.6	26
53	Tungsten trioxide nanoplate array supported platinum as a highly efficient counter electrode for dye-sensitized solar cells. Nanoscale, 2015, 7, 5712-5718.	5.6	22
54	NH3-treated WO3 as low-cost and efficient counter electrode for dye-sensitized solar cells. Nanoscale Research Letters, 2015, 10, 16.	5.7	26

#	Article	IF	CITATIONS
55	High performance NiO microsphere anode assembled from porous nanosheets for lithium-ion batteries. RSC Advances, 2015, 5, 49765-49770.	3.6	29
56	Managing Carrier Lifetime and Doping Property of Lead Halide Perovskite by Postannealing Processes for Highly Efficient Perovskite Solar Cells. Journal of Physical Chemistry C, 2015, 119, 22812-22819.	3.1	123
57	Reduced surface defects of organometallic perovskite by thermal annealing for highly efficient perovskite solar cells. RSC Advances, 2015, 5, 75622-75629.	3.6	66
58	Anatase/TiO ₂ -B hybrid microspheres constructed from ultrathin nanosheets: facile synthesis and application for fast lithium ion storage. CrystEngComm, 2015, 17, 7930-7937.	2.6	18
59	Facile fabrication of MoS2/PEDOT–PSS composites as low-cost and efficient counter electrodes for dye-sensitized solar cells. Journal of Photochemistry and Photobiology A: Chemistry, 2014, 279, 47-51.	3.9	41
60	Morphology control and fabrication of multi-shelled NiO spheres by tuning the pH value via a hydrothermal process. CrystEngComm, 2014, 16, 11096-11101.	2.6	18
61	Electrodeposition of Ag nanosheet-assembled microsphere@Ag dendrite core–shell hierarchical architectures and their application in SERS. CrystEngComm, 2014, 16, 3834-3838.	2.6	17
62	Dye-sensitized solar cells using nanomaterial/PEDOT–PSS composite counter electrodes: Effect of the electronic and structural properties of nanomaterials. Journal of Photochemistry and Photobiology A: Chemistry, 2014, 293, 26-31.	3.9	11
63	Geometric parameter optimization to minimize the light-reflection losses of regular vertical silicon nanorod arrays used for solar cells. Physica Status Solidi (A) Applications and Materials Science, 2014, 211, 2527-2531.	1.8	6
64	A novel hierarchical Pt- and FTO-free counter electrode for dye-sensitized solar cell. Nanoscale Research Letters, 2014, 9, 202.	5.7	15
65	Highly Transparent and Efficient Counter Electrode Using SiO ₂ /PEDOT–PSS Composite for Bifacial Dye-Sensitized Solar Cells. ACS Applied Materials & Interfaces, 2014, 6, 7126-7132.	8.0	66
66	Morphology-controlled synthesis of silver nanoparticles on the silicon substrate by a facile silver mirror reaction. AIP Advances, 2013, 3, .	1.3	15
67	Hydrothermal Synthesis of Anatase TiO2 Nanoflowers on a Nanobelt Framework for Photocatalytic Applications. Journal of Electronic Materials, 2013, 42, 1290-1296.	2.2	29
68	Fabrication of acid-controllable TiO <inf>2</inf> microstructures: Morphology and photocatalytic activity analysis. , 2013, , .		0
69	Synthetized of Ag-doped TiO <inf>2</inf> nanostructures by silver mirror reaction and their photocatalytic activity. , 2013, , .		0
70	SILICON NANOPARTICLES/PEDOT–PSS NANOCOMPOSITE AS AN EFFICIENT COUNTER ELECTRODE FOR DYE-SENSITIZED SOLAR CELLS. Functional Materials Letters, 2013, 06, 1350048.	1.2	8
71	A facile direct deposition of silver nanoparticles on silicon surface by silver mirror process. Crystal Research and Technology, 2013, 48, 1044-1049.	1.3	6
72	New nano-patterns generated by the self-assembling of PS spheres during ICP etching. , 2013, , .		0

#	Article	IF	CITATIONS
73	Porous silicon nanowire arrays with excellent antireflection property. , 2013, , .		Ο
74	Use of delayed electroluminescence as a tool to investigate the emission mechanism of phosphorescent organic light emitting devices. Proceedings of SPIE, 2012, , .	0.8	0
75	Modification of Exciton Lifetime by the Metal Cathode in Phosphorescent OLEDs, and Implications on Device Efficiency and Efficiency Rollâ€off Behavior. Advanced Functional Materials, 2011, 21, 2311-2317.	14.9	42
76	Dependence of carrier recombination mechanism on the thickness of the emission layer in green phosphorescent organic light emitting devices. Organic Electronics, 2011, 12, 582-588.	2.6	25
77	Causes of efficiency roll-off in phosphorescent organic light emitting devices: Triplet-triplet annihilation versus triplet-polaron quenching. Applied Physics Letters, 2010, 97, .	3.3	177
78	Improved UV sensitivity and charge transport in PTB7-Th:PC ₇₁ BM solar cells doped with cadmium selenide quantum dots. Sustainable Energy and Fuels, 0, , .	4.9	3